International Journal of Heat and Mass Transfer 52 (2009) 5271–5275

Contents lists available at ScienceDirect

International Journal of Heat and Mass Transfer

journal homepage: www.elsevier.com/locate/ijhmt

Technical Note

Analysis and optimization of electrokinetic microchannel heat sink

Afzal Husain, Kwang-Yong Kim *

Department of Mechanical Engineering, Inha University, 402-751 Incheon, Republic of Korea

ARTICLE INFO

Article history:
Received 26 September 2008
Received in revised form 9 April 2009
Accepted 27 May 2009

Keywords:
Electroosmosis
Numerical simulation
Microchannel heat sink
Optimization
Pareto-optimal front
Thermal resistance

ABSTRACT

A mixed (electroosmotic and pressure-driven) flow microchannel heat sink has been studied and optimized with the help of three-dimensional numerical analysis, surrogate methods, and the multi-objective evolutionary algorithm. Two design variables; the ratio of the microchannel width-to-depth and the ratio of fin width-to-depth of the microchannel are selected as the design variables while design points are selected through a four-level full factorial design. The single-objective optimization is performed taking overall thermal resistance as the objective function and Radial Basis Neural Network as the surrogate model while for multi-objective optimization pumping power is considered as the objective function along with the thermal resistance. It is observed that the optimum design shifted towards the lower values of the ratio of the channel width-to-depth and the higher values of the ratio of fin width-to-depth of channel with increase of the driving source. The trade-off between the two conflicting objectives has been found and discussed in detail in light of the distribution of Pareto-optimal solutions in the design space. The ratio of channel width-to-depth is found to be higher Pareto-sensitive (sensitivity along the Pareto-optimal front) than the ratio of fin width-to-depth of the channel.

1. Introduction

The last decade has witnessed the development of electroosmotic flow (EOF) capabilities to assist the flow-drive in micro devices used in many industries e.g., medicine and chemical and electronics. Laser and Santiago [1] carried out a survey of micropumps and found that electroosmotic micropumps provide favorable flow rates and pressure head and emerging as a viable option for a number of applications including integrated circuits thermal management, although the working fluid should be electrically inert to avoid any event of accidental leakage [2].

Recent studies found the numerical predictions within the experimental uncertainties, although certain scaling effects can be of different importance for microflows. Mala et al. [3] investigated effects of electric double layer (EDL) field and channel size on the velocity and temperature distribution, streaming potential, apparent viscosity and heat transfer coefficient by solving Poisson–Boltzmann equation. Arulanandam and Li [4] characterized the flow on the basis of cross-section ion concentration and zeta potential using two-dimensional Poisson–Boltzmann and two-dimensional momentum equations in the absence of significant Joule heating. Morini et al. [5] investigated the effect of electroosmotic diameter and geometry aspect ratio on the cross-sectional Nusselt number for trapezoidal and rectangular microchannel heat sinks for a low heat removal rate.

Although, the above studies have characterized thermal transport for EOF, very little attention has been given to three-dimensional numerical simulation of mixed EOF and pressure-driven flow (PDF) microchannel heat sink taking into account temperature dependent fluid properties and Joule heating effects. Recently, the three-dimensional numerical optimization of the microchannel heat sink has been performed under constant pressure and constant pumping power [6] and evolutionary algorithms [7] have been used as the effective tools for generating global Pareto-optimal front in various engineering designs including microchannel heat sinks [8].

The current study explores the application of the surrogate model to optimize the microchannel heat sink for the mixed EOF and PDF. For single-objective optimization, Radial Basis Neural Network (RBNN) [9] as an approximation model with sequential quadratic programming (SQP) implemented in MATLAB [10] are used to find out the optimum solutions. The multi-objective optimization is performed using hybrid multi-objective evolutionary algorithm (MOEA) in combination with three-dimensional Navier–Stokes analysis and a Response Surface Approximation (RSA) [11] model. The global Pareto-optimal front is explored to get inside of the trade-off analysis between the two competing objectives.

2. Geometric and numerical model

The model of the rectangular microchannel heat sink, as shown in Fig. 1, investigated by Husain and Kim [6,8] for PDF has been

* Corresponding author. Tel.: +82 32 872 3096; fax: +82 32 868 1716.
E-mail address: kykim@inha.ac.kr (K.-Y. Kim).

0017-9310/$ - see front matter © 2009 Elsevier Ltd. All rights reserved.
doi:10.1016/j.ijheatmasstransfer.2009.05.028

Nomenclature

A_s	surface area of the substrate base
c_p	specific heat
d_h	hydraulic diameter of the channel
$\boldsymbol{E}$	electric field
e	fundamental electric charge
h_c	microchannel depth
k	thermal conductivity
k_b	Boltzmann constant
k_e	electrical conductivity
l_x, l_y, l_z	length, width and height of the heat sink, respectively
n_∞	ionic number concentration in the bulk solution
P	pumping power
p	pressure
q	heat flux
R_{th}	thermal resistance
T	temperature
$\boldsymbol{u}$	liquid velocity in the microchannel
w_c	width of the microchannel
w_w	fin width
x, y, z	orthogonal coordinate system
z_b	number of valance

Greek symbols

α	design variable, w_c/h_c
β	design variable w_w/h_c
ε	permittivity of the fluid
μ	dynamic viscosity
ρ	density
ρ_e	electric charge density
ψ	electric potential due to charge distribution within the Debye layer

Subscripts

cal	Calorific value
cond	conductive value
conv	convective value
f	fluid
max	maximum value
over	overall value

extended to study the mixed EOF and PDF. In the microfluidics devices when an ionic fluid comes in contact with the charged surface the counter-ions present in the fluid move towards the solid surface and form an EDL, but outside the EDL both co-ions and counter-ions have equal concentrations. The diffuse layer of the EDL is activated and movement of the ions takes place when an external electric field is applied to the microchannel. The balances between the electroosmotic force on the ions and viscous drag force on the fluid in a steady state result in plug-like velocity profile. The electroosmotic force due to electric field is treated as a body force in the Navier–Stokes equations and therefore, resulting governing equations for microchannel can be written as:

$$\text{Momentum}: \quad (\mathbf{u}\cdot\nabla)\rho_f\mathbf{u} = -\nabla p + \nabla.(\mu_f\nabla\mathbf{u}) + \rho_e\mathbf{E} \tag{1}$$

The source term $\rho_e\mathbf{E}$ represents electroosmotic force. The distribution of charge in the EDL describes the net charge density ρ_e. The EDL model of Arulanandam and Li [4] is used to describe the distribution of charge density as:

$$\nabla^2\psi = -\rho_e/\varepsilon \tag{2}$$

Using the equilibrium Boltzmann distribution equation to describe the ion concentration, the charge density for a symmetric electrolyte can be defined as follows:

$$\rho_e = -2n_\infty z_b e \sinh\left(-\frac{z_b e}{k_b T}\psi\right) \tag{3}$$

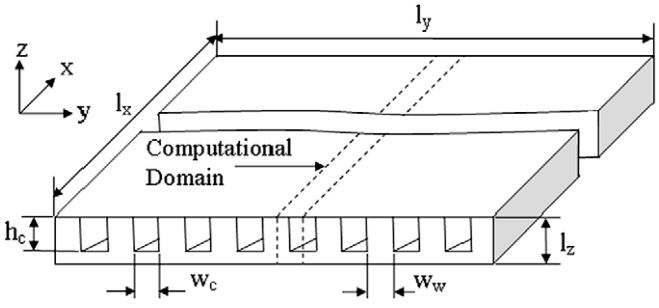

Fig. 1. Schematic of the microchannel heat sink.

The temperature field can be obtained solving following energy equation for fluid:

$$\mathbf{u}\cdot\nabla(\rho_f c_{pf} T_f) = \nabla\cdot(k_f\nabla T_f) + E^2 k_e \tag{4}$$

No-slip ($\mathbf{u} = 0$) boundary conditions are applied at the channel walls. Pressure boundary conditions are applied at the inlet and exit of the microchannel heat sink. The electric potential at the channel walls is assigned equal to the zeta potential as 0.2 V. The flow is assumed to be steady and laminar and a uniform heat flux is applied at the bottom of the heat sink. The numerical simulations are carried out using a commercial finite volume solver CFX 11.0 [12] having Semi-Implicit Method for Pressure Linked Equations (SIMPLE) algorithm [13] for pressure correction. Thermophysical and electrical properties [14,15] of the coolant liquid (water) are allowed to vary with temperature [8] and Joule heating and viscous dissipation have been included to take into account the micro-scales effects.

3. Optimization techniques

The shape of the microchannel is optimized by constructing two design variables i.e., α and β, where α is defined as w_c/h_c and β is defined as w_w/h_c. A four-level full factorial design is used to exploit the design space with limits $0.1 \leqslant \alpha \leqslant 0.25$ and $0.04 \leqslant \beta \leqslant 0.1$.

The heat transfer performance of the microchannel heat sink is studied in terms of overall thermal resistance and pumping power which are set as objective functions to minimize. The overall thermal resistance for a fully developed flow microchannel heat sink is defined as:

$$R_{th,over} = R_{th,cond} + R_{th,conv} + R_{th,cal} = \frac{\Delta T_{\max}}{qA_s} \tag{5}$$

The pumping power required to drive the fluid through microchannel heat sink can be defined as [6]:

$$P = \frac{nA_c d_h^2 \Delta p^2}{2\gamma\mu l_x} \tag{6}$$

Here n is the number of microchannels, A_c is the cross-section area and γ is the friction factor of the microchannel.

The objective functions, viz., thermal resistance and pumping power, are evaluated numerically at the designed sites at various levels of pressure drop and electric field. For the detail of the opti-

mization procedure readers can refer to Husain and Kim [6,8]. The surrogate model, RBNN is trained using the discrete numerical solutions in the design space for single-objective (thermal resistance) optimization. The response of the RBNN is checked through leave-one-out cross-validation which is also known as PRESS (Prediction Error Sum of Squares) in the polynomial response surface terminology [11]. In the microchannel heat sink an increase in applied pumping source leads to decrease in thermal resistance. This exhibits competing nature of thermal resistance and pumping source which requires simultaneous optimization of both the objective functions. The multi-objective optimization requires objective function values at many locations to find out the Pareto-optimal solutions. Therefore, to avoid numerical expenses RSA methodology is applied to predict the objective function values anywhere in the design space. A hybrid multi-objective evolutionary approach is used to obtain global Pareto-optimal solutions [7]. In this method first Pareto-optimal solutions are obtained with the help of real coded NSGA-II (Non-dominated Sorting Genetic Algorithm-II) [7] for two objective functions; thermal resistance and pumping power. These Pareto-optimal solutions are then refined by searching a local optimal solution for each objective function over the whole NSGA-II obtained optimal solutions using SQP with NSGA-II solutions as initial guesses. The representative solutions out of the global Pareto-optimal solutions are found out by applying k-means clustering algorithm [16].

4. Results and discussion

A $121 \times 25 \times 61$ unstructured hexahedral grids is used for the fluid domain with a total of 252000 elements (for both fluid and solid) for a typical design; $\alpha = 0.175$ and $\beta = 0.075$ for both EOF and PDF after carrying out a grid independency test. The numerical solutions are converged below a residual value of 10^{-6} for electric potential, velocity, pressure and temperature. It was found that for a $145 \times 41 \times 97$ grid with a total of 660000 elements the change in Nusselt number was about 1% while for $101 \times 18 \times 44$ grid with a total 147500 elements the change in Nusselt number was more than 3%. The validation of the pure PDF has been reported in the previous study by Husain and Kim [6,8]. The further validation of pure PDF and pure EOF has been performed and the solutions are compared for the flow rate and Nusselt number with the analytical [4,17,18] and numerical [5] results as shown in Fig. 2.

The values of design parameters of the RBNN namely Spread Constant (SC) and Error Goal (EG) are set 0.2 and 5.0×10^{-5}, respectively, for a typical case of driving source $\Delta p = 10$ kPa and $E_x = 10$ kV/cm. The optimum design of the microchannel is searched with the help of constructed RBNN and SQP at various source values of pressure head and electric field as shown in Table 1. The higher values of α leads to the higher flow rate due to electroosmosis which results in lower caloric thermal resistance. The thermal resistance due to convection is inversely proportional to the heat transfer coefficient (h) and area subjected to convective heat transfer ($A_{s,f}$). Furthermore, the area subjected to convective heat transfer is directly proportional to α for a fixed value of microchannel length (l_x) and height (h_c). Therefore, increase of mean fluid velocity (u_{avg}) or α leads to decrease overall thermal resistance due to lower convective thermal resistance. For mixed flow at lower pressure head the optimum point lie at the higher value of α and it shows almost no variation with increase of electric field. On the other hand, increase of pressure head leads to the increase of mean velocity which reduces the convection thermal resistance as well as caloric thermal resistance. Therefore with increase of pressure head the optimum design shifts towards the lower value of α. The optimum design is found near the higher value of α under the limited pressure head value. At higher pressure head values the optimum design shifted towards the lower value of α and higher value of β within the design space explored.

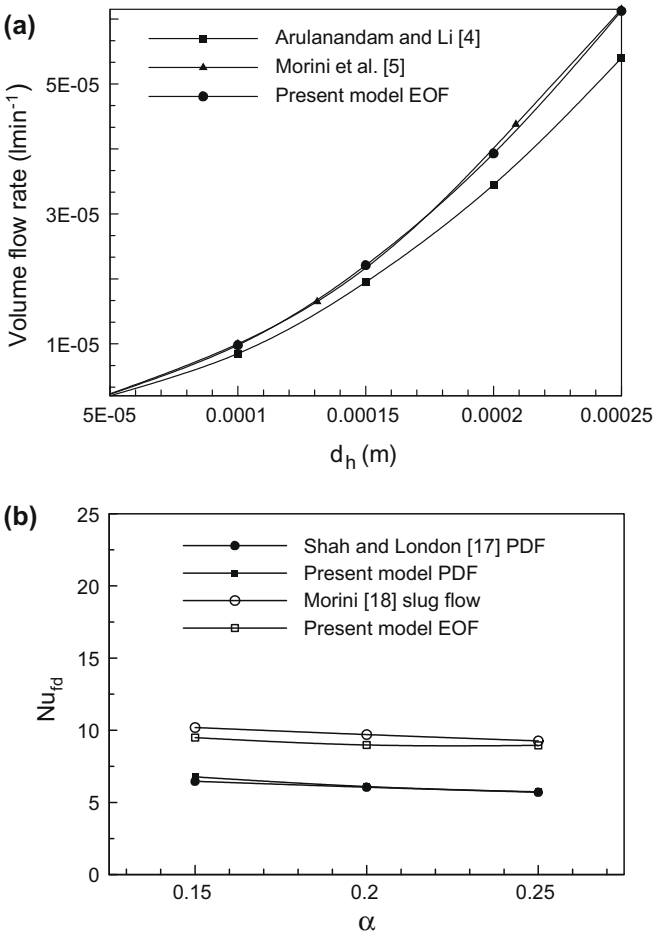

Fig. 2. Comparison of present numerical results with analytical and previous numerical solutions: (a) flow rate at pure EOF and (b) fully developed Nusselt number at pure PDF and pure EOF.

The above study shows the dependency of the optimum design to pressure head and electric field. Therefore for global optimization of the microchannel heat sink both pressure head and electric field should be considered as objective functions along with the overall thermal resistance. This gives rise to a problem of multi-objective optimization. The micropump pressure-discharge characteristics further added complexity to the optimization of microchannel heat sink and its realization to practical design. In this line a multi-objective optimization of the microchannel heat sink has been performed in this study taking pumping power and thermal resistance as objective functions. For a typical case covered in the present work pressure head and electric field applied at the inlet of the microchannel heat sink are set 10 kPa and 10 kV/cm, respectively.

Table 1
Design variables at different optimum points obtained at changing pumping source.

Δp (kPa)	E_x (kV/cm)	α	β	R_{th} (K/W)
7.5	10	0.250	0.060	0.1865
7.5	15	0.250	0.062	0.1799
7.5	20	0.250	0.062	0.1776
10	10	0.249	0.078	0.1703
15	15	0.185	0.066	0.1435

The analysis of variance and regression analysis provided by t statistics [11] are implemented to measure the uncertainties in the sets of coefficients of the polynomials in the RSA models. The values of R^2, R^2_{adj} and root mean PRESS are kept 0.993, 0.989 and 7.37e−3, respectively for thermal resistance and 0.999, 0.998 and 5.37e−5, respectively for pumping power. The present study applies the model of MOEA used by Husain and Kim [8]. A real coded NSGA-II is invoked to obtain well spread approximate Pareto-optimal solutions with 250 generations 100 populations. The crossover and mutation probabilities are set to 0.85 and 0.2, respectively. The crossover and mutation parameters are decided as 15 and 150, respectively. These parameters are adjusted one by one to suit the nature of the problem. After a local search, there are 679 optimal solutions which are called as global Pareto-optimal solutions. Five representative clusters are formed applying K-means clustering as shown in Fig. 3 along with the NSGA-II and global Pareto-optimal solutions. The shape of the Pareto-optimal front obtained by hybrid MOEA is concave in nature which suggests the competing nature of the two objective functions as shown in Fig. 3(a). The improvement of one objective functions leads to the deterioration of the other objective function. Lower thermal resistance is obtained at higher pumping power and vice versa. It can be concluded that no solution out of the 679 Pareto-optimal solutions is superior to other in both objectives since each solution is global Pareto-optimal solution.

The sensitivity analysis of the design variables along the Pareto-optimal front is performed by plotting the design variables corresponding to the five clusters. The characteristic variation of the design variables along the Pareto-optimal front corresponding to the cluster points is shown in Fig. 3(b). This analysis gives designer a freedom to economically choose the combination of the design variables and their corresponding objective functions. It is observed that α shows continuously increasing characteristic while β shows alternating decreasing and increasing characteristic with increase of pumping power along the Pareto-optimal front. Although both of the two design variables are Pareto-sensitive (variation of the design variables along the Pareto-optimal front) and their values change with a change in pumping power, design variable α is found to be more Pareto-sensitive than β.

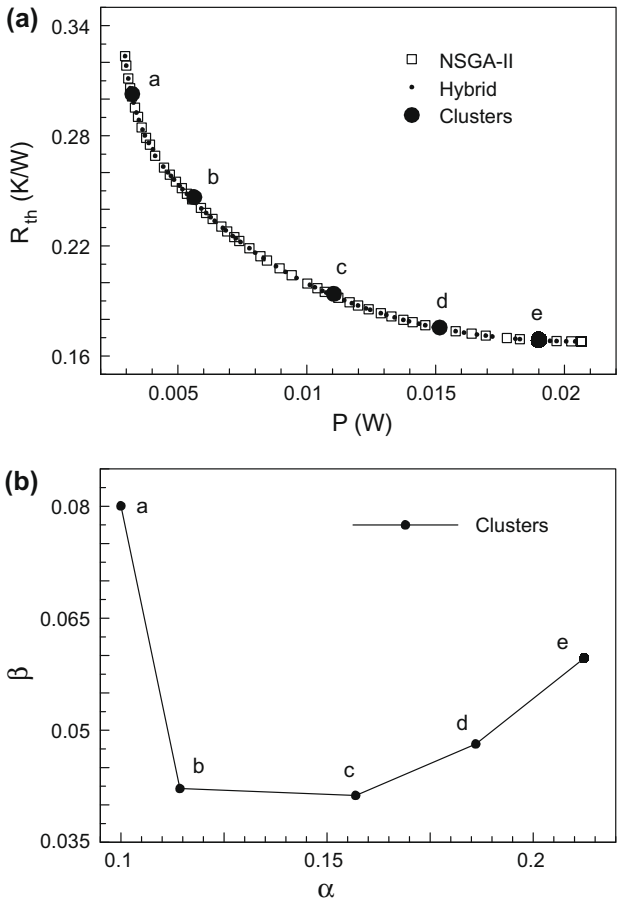

Fig. 3. (a) Pareto-optimal front for thermal resistance and pumping power. (b) Distribution of design variables along the Pareto-optimal front.

5. Conclusion

The present study demonstrates the model of the optimization of electroosmotically assisted pressure-driven microchannel heat sink. The electroosmosis can be efficiently used to assist the driving source to enhance the performance of the microchannel heat sink. Two design variables related to the microchannel width, depth and fin width are defined and the design points are selected using four-level full factorial design. The numerical solutions at these design points are obtained to construct surrogate models, viz., Radial Basis Neural Network and Response surface Approximation. The optimum design is found to shift towards the lower values of the channel width-to-depth ratio and higher values of the fin width-to-depth ratio of the microchannel with increase of driving source. Global Pareto-optimal front is obtained using hybrid multi-objective evolutionary algorithm which shows existing trade-off. The ratio of the channel width-to-depth is found to be higher Pareto-sensitive (variation of the design variables along the Pareto-optimal front) than the ratio of fin width-to-depth of the microchannel. The trade-off between objective functions and Pareto-sensitivity of the design variables can be utilized to economically design the microchannel heat sink.

Acknowledgement

This research was supported by INHA UNIVERSITY Research Grant.

References

[1] D.J. Laser, J.G. Santiago, A review of micropumps, J. Micromech. Microeng. 14 (2004) R35–R64.
[2] Y. Joshi, X. Wei, Micro and meso scale compact heat exchangers in electronics thermal management – a review, in: R.K. Shah, M. Ishizuka, T.M. Rudy, V.V. Wadekar (Eds.), Proceedings of Fifth International Conference on Enhanced, Compact and Ultra-Compact Heat Exchangers: Science, Engineering and Technology, Engineering Conferences International, Hoboken, NJ, USA, 2005.
[3] G.M. Mala, D. Li, J.D. Dale, Heat transfer and fluid flow in microchannels, Int. J. Heat Mass Transfer 40 (13) (1997) 3079–3088.
[4] S. Arulanandam, D. Li, Liquid transport in rectangular microchannels by electroosmotic pumping, Colloids Surf. A: Physicochem. Eng. Aspects 161 (2000) 89–102.
[5] G.L. Morini, M. Lorenzini, S. Salvigni, M. Spiga, Thermal performance of silicon micro heat-sinks with electrokinetically-driven flows, Int. J. Therm. Sci. 45 (2006) 955–961.
[6] A. Husain, K.-Y. Kim, Shape optimization of micro-channel heat sink for micro-electronic cooling, IEEE Trans. Compon. Pack. Technol. 31 (2) (2008) 322–330.
[7] K. Deb, Multi-Objective Optimization Using Evolutionary Algorithms, first ed., John Wiley & Sons Inc, 2001.
[8] A. Husain, K.-Y. Kim, Optimization of a microchannel heat sink with temperature dependent fluid properties, Appl. Therm. Eng. 28 (2008) 1101–1107.
[9] M.J.L. Orr, Introduction to Radial Basis Neural Networks, Center for cognitive science, Edinburgh University, Scotland, UK, 1996, http://anc.ed.ac.uk/RBNN/.
[10] MATLAB®, The Language of Technical Computing, Release 14, The Math Works Inc., 2004.
[11] R.H. Myers, D.C. Montgomery, Response Surface Methodology: Process and Product Optimization using Designed Experiments, John Wiley & Sons, Inc., NY, 1995.
[12] CFX-11.0, Solver Theory, 2006, ANSYS.

[13] S.V. Patankar, Numerical Heat Transfer and Fluid Flow, McGraw-Hill, NY, 1980.
[14] F.P. Incropera, D.P. DeWitt, Fundamentals of Heat and Mass Transfer, John Wiley & Sons Inc, New York, 2002.
[15] X. Xuan, D. Sinton, D. Li, Thermal end effects on electroosmotic flow in a capillary, Int. J. Heat Mass Transfer 47 (2004) 3145–3157.
[16] JMP, The Statistical Discovery Software, version 6, SAS Institute Inc., Cary, NC, USA, 2005.
[17] R.K. Shah, A.L. London, Laminar flow forced convection in ducts, in: Adv. Heat Transfer (Suppl. 1), Academic Press, New York, 1978.
[18] G.L. Morini, Thermal characteristics of slug flow in rectangular ducts, Int. J. Therm. Sci. 38 (1999) 148–159.